HYDROLOGICAL PROCESSES
Hydrol. Process. **22**, 3919–3930 (2008)
Published online 13 May 2008 in Wiley InterScience
(www.interscience.wiley.com) DOI: 10.1002/hyp.7029

Seasonal waves on glaciers

I. J. Hewitt[1]* and A. C. Fowler[2]

[1] *Mathematical Institute, Oxford University, 24-29 St Giles', Oxford OX1 3LB, UK*
[2] *Department of Mathematics and Statistics, University of Limerick, Limerick, Republic of Ireland and Mathematical Institute, Oxford University, 24-29 St Giles', Oxford OX1 3LB, UK*

Abstract:

Seasonal waves accompanying annual changes in the sliding velocity of ice travel down glacier at speeds much faster than the ice itself. A simple explanation for these waves in terms of the passage of a pressure wave through the subglacial drainage system is given. Drainage by both distributed and localized systems is explored, with the sliding velocity governed by a dependence on the effective pressure. Waves are caused by drainage through a slow distributed system, but may be damped if this is well connected to an efficient channelized system. A possible connection between these waves and high velocity spring events is discussed. Copyright © 2008 John Wiley & Sons, Ltd.

KEY WORDS subglacial hydrology; glacier sliding; glacier dynamics; seasonal drainage evolution

Received 8 September 2007; Accepted 7 February 2008

INTRODUCTION

Waves on glaciers have been observed for over 100 years. The theory of *kinematic* waves has been well developed by Weertman (1958); Nye (1960); Weertman and Birchfield (1983), and can account for observed bulges in the surface of the ice that travel downglacier at around 5 times the ice velocity. An altogether different type of wave, however, is a perturbation in the ice velocity itself. Such waves, termed *Druckwellen*, were apparently well known on the Hintereisferner at the beginning of the last century, travelling between 20 and 150 times as fast as the ice itself (Blümcke and Finsterwalder, 1905; Deeley and Parr, 1914). This type of wave on the Hintereisferner was also documented in the 1950s (Schimpp, 1958; Finsterwalder, 1961), and perhaps the best example is seen on Nisqually glacier in the detailed velocity measurements made by Hodge (1974). These waves appear to be associated with annual speed-up of the glacier and have therefore been described as *seasonal waves*. Unfortunately, more recent and widespread observations of them are lacking and, perhaps because of this, they have received little attention. This article explores a simple theory that may explain these waves due to kinematic waves in the subglacial drainage system.

Our main aim is to reproduce some of the qualitative features of Hodge's measurements, which are summarized in Figure 1. These show large increases in the surface velocity of the glacier during the summer at all points in the ablation area. The timing of the peak velocity during the summer and the minimum velocity during the winter is about 1 month later towards the terminus than near the equilibrium line, and this progressive shift represents the seasonal wave that Hodge estimates to be travelling at around 20 km a^{-1}. There is no associated surface elevation change, and the presumption is that the large seasonal velocity variations, and consequently the seasonal wave, are due to changes in the slip of the glacier at its bed.

The velocity changes occurring here appear to be distinct from so-called 'spring events' (Iken and Bindschadler, 1986; Copland *et al*., 2003; Willis *et al*., 2003; Anderson *et al*., 2004) or 'mini-surges' (Kamb and Engelhardt, 1987) when a period of fast sliding accompanied by high borehole water pressures occurs during the spring, and after which sliding velocities reduce to a more steady summer value. Such events have been observed to travel rapidly either up or downglacier. Unlike these, however, the seasonal wave we consider is a longer-lived feature involving the passage of a mid-season maximum.

SLIDING LAWS

The motion of a temperate glacier can be separated into a component u_i due to internal plastic deformation of the ice and a component u_b due to sliding of the ice over its bed. The internal component may be described most simply with the shallow ice approximation (Paterson, 1994),

$$u_i = \frac{2A}{n+1}\tau_b^n H \qquad \tau_b = \rho_i g H \sin\alpha_s \tag{1}$$

Here, A and n are the usual coefficients in Glen's flow law for ice, H is the depth of the ice, and τ_b is the basal shear stress that must balance the driving stress produced by the glacier slope α_s. Variations in the glacier depth clearly cause variations in velocity (Nye,

* Correspondence to: I. J. Hewitt, Mathematical Institute, Oxford University, 24-29 St Giles', Oxford OX1 3LB, UK.
E-mail: hewitt@maths.ox.ac.uk

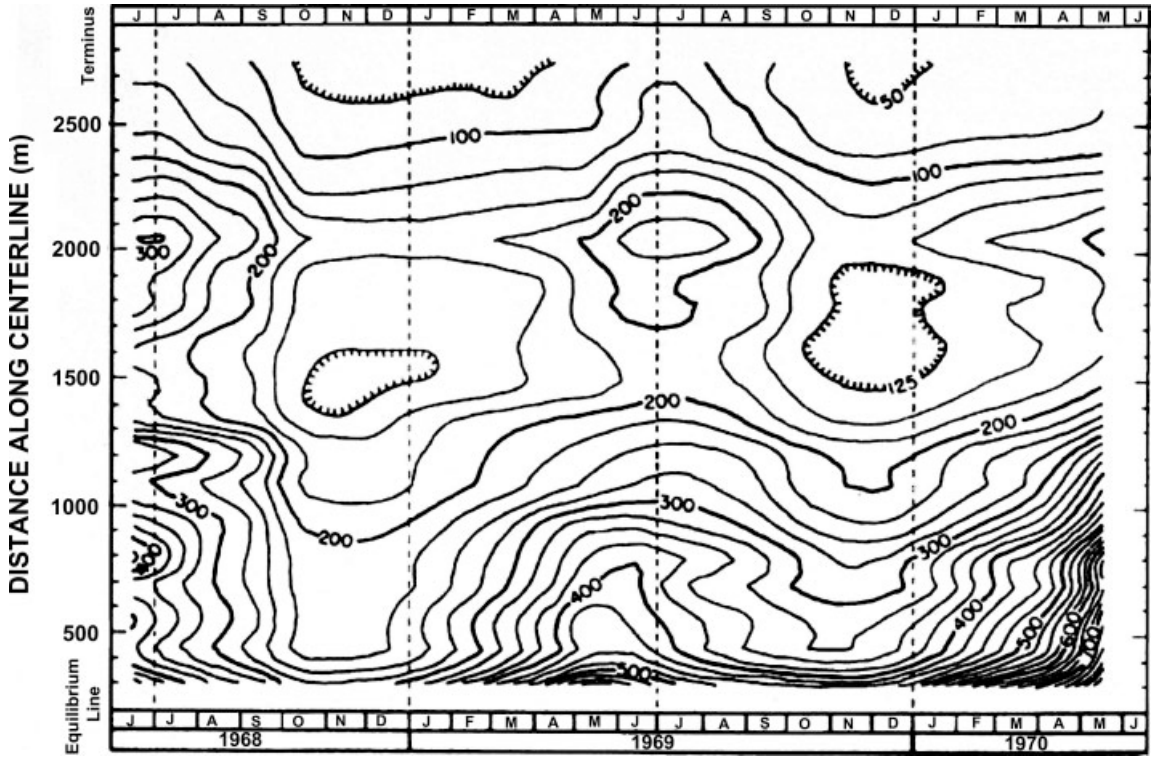

Figure 1. Measured surface speed of Nisqually Glacier, Mt. Rainier, Washington, as a function of distance and time. Contour interval is 25 mm d^{-1}. Reproduced from Hodge, 1974

1960), but not nearly enough, nor at the right time, to account for observed seasonal changes (Hodge, 1974). Seasonal variations must therefore be associated with changes in the basal sliding velocity and presumably with the amount of water present at the bed (Willis, 1995; Jansson, 1996).

Temperate and polythermal glaciers can slide over their bed by a combination of regelation and enhanced plastic flow over bedrock bumps (Weertman, 1957), and by the deformation of a layer of subglacial till. The presence of pressurized meltwater causes the ice to separate from its bed in places (Lliboutry, 1968), and the resulting cavities reduce the contact area and hence friction between the ice and the bed. Theoretical models of sliding over a rough bed with cavitation suggest a friction law of the form

$$\frac{\tau_b}{N_C} = f\left(\frac{u_b}{N_C^n}\right) \tag{2}$$

relating the sliding velocity u_b to basal shear stress τ_b and effective pressure in the cavities $N_C = p_i - p_w$ (Nye, 1969; Fowler, 1986; Schoof, 2005). For small enough values of its argument the function f is increasing, and may be well represented by

$$f(\Lambda) = \Lambda^{1/m} \tag{3}$$

The sliding law can then be written in the power-law form

$$u_b = c\tau_b^p N_C^{-q} \tag{4}$$

with p, $q > 0$. Empirical laws of this form, in which the constant c depends upon the roughness of the bed, are commonly used as the basal boundary condition for glacier flow models and also have some experimental foundation (Budd *et al*., 1979). Commonly used values for p range between 1 and 4, while q is typically about 1 so that the sliding velocity varies inversely with the effective pressure. Such a dependence has been established on a number of temperate glaciers (Iken and Bindschadler, 1986; Jansson, 1996), and we will base our sliding model on (4), concentrating particularly on the N_C dependence.

DRAINAGE MECHANISMS

Subglacial drainage mechanisms can be broadly classified as localized or distributed, the former characterized by efficient, well-developed flow paths with low water pressure, the latter by inefficient poorly connected drainage at high water pressures. The type of drainage that occurs may depend upon factors such as the amount of meltwater produced, the nature of the glacier bed, and the direction and magnitudes of potential gradients within the glacier. Seasonal evolution of drainage systems is well documented (Brzozowski and Hooke, 1981; Hooke, 1989; Nienow *et al*., 1998; Copland *et al*., 2003; Willis *et al*., 2003), and any one glacier may have very different drainage properties depending on the time of year.

We will discuss drainage through two systems; an arborescent network of R-channels and a distributed system of linked cavities. In the channel drainage theory developed by Röthlisberger (1972); Shreve (1972); Nye

DOI: 10.1002/hyp

(1976); Spring and Hutter (1982), the conduit size is governed by the competing processes of viscous dissipation melting the ice walls and viscous closure of the ice due to the difference between the overburden ice pressure p_i and the water pressure p_w. In the steady state this leads to a relationship

$$N_R = \left(\frac{Q_R}{\gamma_R}\right)^{1/4n} \mathcal{G}_R^{11/8n}$$

$$\mathcal{G}_R = |-\nabla(\rho_i g z_s + (\rho_w - \rho_i) g z_b - N_R)| \qquad (5)$$

between the effective pressure $N_R = p_i - p_w$, the water flux through the channel Q_R, and the gradient of the water potential, $\mathcal{G}_R$. Here, z_s and z_b are the elevation of the glacier surface and bed, ρ_w and ρ_i are the densities of water and ice, and γ_R is a constant. The cross-sectional area S_R of the channel depends upon the effective pressure and potential gradient,

$$S_R = \beta_R N_R^{3n} \mathcal{G}_R^{-9/2} \qquad (6)$$

in which β_R is another constant. The effective pressure is larger for a larger water flux, which gives the property that larger channels, having lower water pressure, tend to capture water from their smaller neighbours. These channels, if they exist, are therefore supposed to form an arborescent network branching up the glacier.

Linked cavity drainage was first suggested by Lliboutry (1969) and later more fully developed in an attempt to explain glacier surge mechanisms (Walder, 1986; Fowler, 1987; Kamb, 1987). Cavities are formed as a result of ice sliding over bedrock bumps, but they also influence the rate of sliding, and this feedback means their dynamics and evolution are not straightforward. The basic mechanism governing cavity evolution is the balance between opening by sliding and closure by viscous deformation of the ice. The meltback of the ice walls has only a secondary opening effect, and this fact distinguishes the cavities from Röthlisberger channels. The governing balance leads to a relationship (Walder, 1986) of the form

$$S_C = \beta_C \frac{u_b}{N_C^n} \qquad (7)$$

between the cross-sectional area S_C of cavities (across the glacier), the sliding velocity u_b, and the effective pressure $N_C = p_i - p_w$. The water flux through these interconnected cavities is

$$Q_C = \gamma_C \frac{u_b}{N_C^n} \mathcal{G}_C^{1/2}$$

$$\mathcal{G}_C = |-\nabla(\rho_i g z_s + (\rho_w - \rho_i) g z_b - N_C)| \qquad (8)$$

Combining (4), (8) and (7) gives

$$S_C = c\beta_C \tau_b{}^p N_C{}^{-(n+q)} \qquad Q_C = c\gamma_C \tau_b{}^p N_C{}^{-(n+q)} \mathcal{G}_C^{1/2} \qquad (9)$$

In this case, the effective pressure is lower for larger water flux, so that there is no tendency for capture of water and the cavities remain distributed across the bed.

The basic situation we consider is that of a model parallel slab glacier, with uniform height and slope. The basal shear stress in (9) can then be taken as constant. This simplification is made to elucidate the ideas without the extra complications of spatial and temporal changes in shear stress. Although idealistic, this may, in fact, be a reasonable approximation to make for the case of Nisqually glacier, which is about as uniform as one could hope for a real glacier, and where in any case there is no obvious correlation between sliding velocity and shear stress (Meier, 1968; Hodge, 1974).

We make the assumption that gravity is the principal potential gradient driving water flow downglacier, so we ignore the effective pressure gradients in the water potentials. We therefore take $\mathcal{G}_R = \mathcal{G}_C = \mathcal{G}_0 \equiv \rho_w g \sin \alpha_s$ to be constant, with α_s as the surface slope. This is a singular approximation that can be expected to break down near the glacier margins, but which significantly simplifies the governing equations for flow under the bulk of the glacier. Equations (5) and (9) are then simply algebraic relationships between the effective pressure and water flux carried by the drainage system, and are shown in Figure 2.

For the purposes of this study, we are interested only in certain properties of each drainage system that are contained in the expressions (5), (6) and (9). We have concentrated on Röthlisberger channels and linked cavities to arrive at these governing relationships, but other types of drainage result in very similar relationships with the distinction being the differing $N - Q$ dependence shown in Figure 2. References to Röthlisberger channels and linked cavities in the remainder of this article may therefore be thought of more generally as any type of localized and distributed system, respectively. In particular, the ideas here should still apply for soft-bedded glaciers when drainage may occur through a distributed canal system (e.g. Walder and Fowler, 1994), and the sliding caused by deformation of the till is expected to depend on the pore pressure in much the same way as in (4).

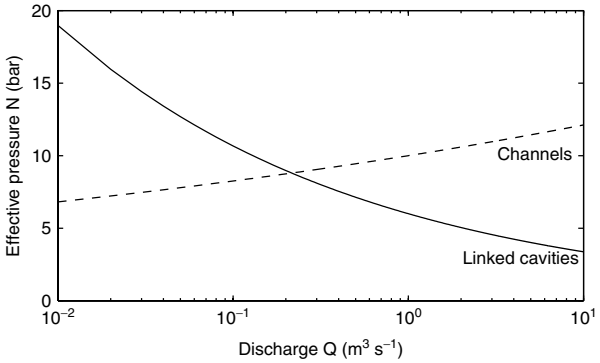

Figure 2. Variation in steady state effective pressure N with discharge Q for R-channels (dashed) and linked cavities (solid), for the case of constant gravitational potential gradient as given by (5) and (9)

DOI: 10.1002/hyp

DRAINAGE MODEL

Motivation - linked cavity drainage

The basis of the model we consider is the continuity equation for subglacial meltwater,

$$\frac{\partial S}{\partial t} + \frac{\partial Q}{\partial x} = M \tag{10}$$

The glacier is treated as one dimensional, with x as the coordinate along the centreline in the downglacier direction. S is the cross glacier sectional area of the drainage system and Q is the water flux carried through that system in the downglacier direction. M ($m^2\ s^{-1}$) is the meltwater input, which is taken to be the lumped sum of water derived from surface melting and run off, englacial storage and basal melting.

Equation (10) is a kinematic wave equation and we can expect variations in the meltwater source term to cause perturbations in the water flux that propagate as waves. The speed of the waves will be comparable to the speed of the water, and the relationships between discharge and effective pressure show that there are accompanying waves in the water pressure.

Suppose first that drainage occurs through a linked cavity system. From (7) and (8) the discharge is proportional to the cross-sectional area, so we can write

$$\alpha\frac{\partial Q_C}{\partial t} + \frac{\partial Q_C}{\partial x} = M \tag{11}$$

with $\alpha = \beta_C/\gamma_C\mathcal{G}_0^{1/2}$. A simple annually varying meltwater input is sinusoidal and independent of position on the glacier.

$$M = M_0(1 + \cos\omega t) \tag{12}$$

with $\omega = 2\pi y^{-1}$ so that $t = 0$ is the time of maximum melt, and with the boundary condition $Q_C = 0$ at $x = 0$, the solution is straightforward;

$$Q_C = M_0 x + \frac{2M_0}{\omega\alpha}\cos\omega\left(t - \frac{\alpha}{2}x\right)\sin\omega\left(\frac{\alpha}{2}x\right) \tag{13}$$

From this simple solution it is clear that the varying melt input causes waves in the water flux, and the maximum water flux propagates downglacier at speed $2/\alpha$. The algebraic relationships (4) and (9) then give the sliding velocity

$$u_b = \left(\frac{c^n \tau_b^{np}}{\gamma_c^q \mathcal{G}^{q/2}}\right)^{1/(n+q)} Q_C^{q/(n+q)} \tag{14}$$

which varies exactly in phase with the cavity flux, as shown in Figure 3 for a 2-year period. This is of course a rather over-simplified picture of sliding and meltwater interaction, but it does quite clearly show the possibility for waves in the sliding velocity to propagate downglacier.

Coupled drainage systems

There is strong evidence, from dye tracing, borehole pressure and surface uplift measurements, that drainage occurs by both distributed linked cavities and well connected channels (Hooke, 1989; Hock and Hooke, 1993; Nienow *et al.*, 1998). We therefore consider a two-component drainage model in which both types of drainage operate in parallel. The situation envisaged is of a large cavity covered bed intersected by a branching network of channels. Water will be assumed to reach the bed distributed across the whole glacier. It moves slowly downglacier through the linked cavity system, but preferentially moves into the channel system because the water pressure is lower there. Once in the channel

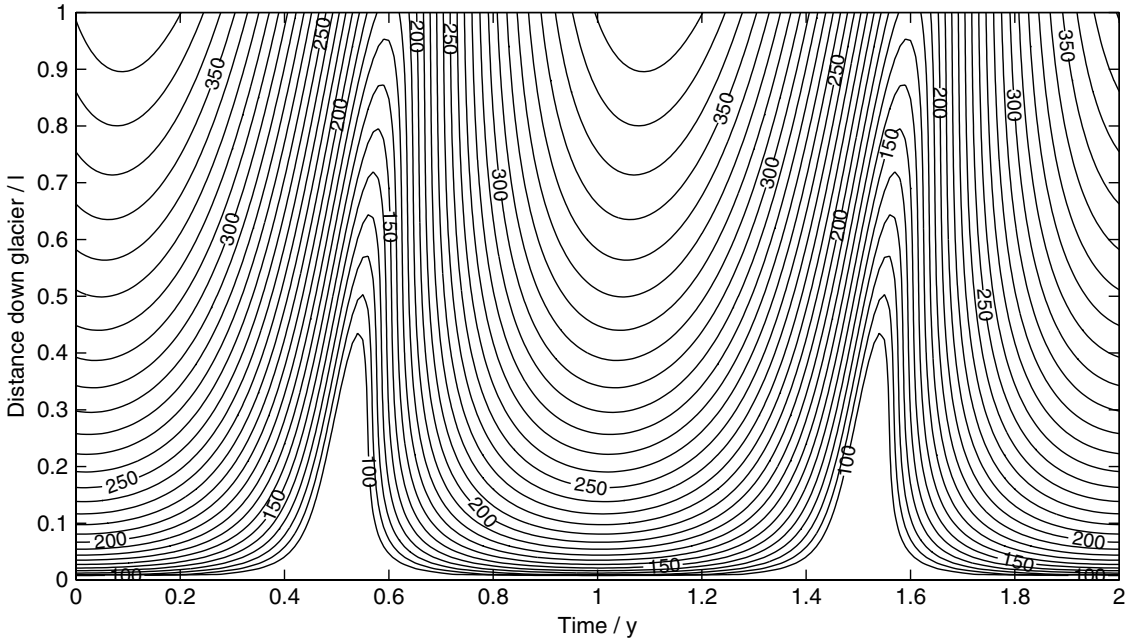

Figure 3. Contour plot of sliding velocity variations driven by changes in water pressure in a linked cavity system, as given by (13) and (14), with $\alpha = 0{\cdot}2$. Contour interval is 10 mm d^{-1}

DOI: 10.1002/hyp

network the water is rapidly and efficiently routed out of the glacier.

The governing equations are a modification of (10) for each drainage system:

$$\frac{\partial S_C}{\partial t} + \frac{\partial Q_C}{\partial x} = M_C - L(N_R, N_C) \tag{15}$$

$$\frac{\partial S_R}{\partial t} + \frac{\partial Q_R}{\partial x} = M_R + L(N_R, N_C) \tag{16}$$

where the subscripts C and R refer to linked cavities and R-channels, respectively. The coupling term L denotes the leakage of water from cavities to channels and is a function of the effective pressure difference between the two systems. The simplest choice for L is that it is directly proportional to the pressure difference,

$$L = k(N_R - N_C) \tag{17}$$

The proportionality constant k can be estimated from the rate of flow down a potential gradient through a linked cavity system, with the width of the glacier W used as a suitable length scale (cf. Flowers *et al.*, 2004). Separate meltwater inputs are included to the two drainage systems, but in most of what follows, we will suppose that $M_R = 0$ and that all the meltwater reaches the glacier bed in the distributed system. The channels at the bed are considered as very localized structures so that the vast majority of the bed area is covered by cavities and it is therefore natural to suppose that the majority of the melt might enter this system (Raymond *et al.*, 1995). It is also common that water routed from the glacier surface through crevasses and moulins may collect together englacially so that by the time it reaches the bed it is already in an efficient conduit that feeds straight into the channel network at the bed. Such water routing can be catered for by including non-zero M_R, but turns out to have relatively little effect on our results.

The three variables S, Q and N for each system are related by the simple algebraic relationships in (5), (6), (7) and (8).

The sliding velocity is given by the sliding law (4), in terms of the effective pressure in the cavities. The choice to use the cavity pressure in the sliding law rather than the channel pressure is due to the fact that cavities cover the majority of the bed, and indeed it is the presence of the cavities that influences the sliding rate.

Non-dimensionalization

Equations (15), (16), (5), (6), (7) and (8) are non-dimensionalized in a standard way by defining

$$x = lx^* \quad S_C = S_{C0}S_C^* \quad Q_C = Q_0Q_C^* \quad N_C = N_0N_C^*$$
$$t = t_0t^* \quad S_R = S_{R0}S_R^* \quad Q_R = Q_0Q_R^* \quad N_R = N_0N_R^* \tag{18}$$

where $Q_0 = M_0l$ is the scale for the water flux in terms of melt input scale M_0 (externally prescribed by the glacier's climate and topography) and glacier length l. The pressure scale N_0 is chosen from (5) to be

$$N_0 = \gamma_R^{-1/4n}\mathcal{G}_0^{11/8n}Q_0^{1/4n} \tag{19}$$

and the cross-sectional areas from (9) and (6),

$$S_{C0} = \frac{\beta_C}{\gamma_C\mathcal{G}_0^{1/2}}Q_0 \quad S_{R0} = \beta_RN_0^{3n}\mathcal{G}_0^{-9/2} \tag{20}$$

Since we are interested in looking at seasonal variations we set the timescale of interest t_0 to be 1 year.

On dropping the asterisks, the resulting set of non-dimensional equations is

$$\alpha_C\frac{\partial S_C}{\partial t} + \frac{\partial Q_C}{\partial x} = M_C - \kappa(N_R - N_C) \tag{21}$$

$$\alpha_R\frac{\partial S_R}{\partial t} + \frac{\partial Q_R}{\partial x} = M_R + \kappa(N_R - N_C) \tag{22}$$

$$S_C = Q_C \quad N_C = \delta Q_C^{-1/(n+q)} \tag{23}$$

$$S_R = Q_R^{3/4} \quad N_R = Q_R^{1/4n} \tag{24}$$

The parameters are

$$\alpha_C = \frac{1}{t_0}\frac{\beta_C}{\gamma_C\mathcal{G}_0^{1/2}} \quad \alpha_R = \frac{1}{t_0}\frac{\beta_R}{\gamma_R^{3/4}Q_0^{1/4}\mathcal{G}_0^{3/8}}$$
$$\delta = \frac{c^{1/(n+q)}\gamma_C^{1/(n+q)}\gamma_R^{1/4n}\tau_b^{p/(n+q)}}{\mathcal{G}_0^{(7n+11q)/8n(n+q)}Q_0^{(5n+q)/4n(n+q)}}$$
$$\kappa = \frac{k\mathcal{G}_0^{11/8n}Q_0^{1/4n}}{\gamma_R^{1/4n}M_0} \tag{25}$$

and these represent, respectively, the advective timescales in years for cavity and channel drainage, the ratio of typical effective pressures in a cavity system to those in a channel system, and the non-dimensional coefficient of proportionality in the leakage term, which may be thought of as representing the 'connectedness' of the two drainage systems (cf. Flowers *et al.*, 2004).

The various constants in (5), (6), (7), (8) and (4) depend on a number of uncertain parameters, particularly the Manning's roughness coefficient, the roughness of the glacier bed, and the tortuosity and connectedness of flow paths in the linked cavities. The suitable values given in Table I may be considered representative of reasonable choices for these parameters, but, in fact, it

Table I. Values of model constants

Constant	Value
n	3
p	4
q	1
c	2×10^{-20} m s^{-1} Pa^{-3}
γ_R	$1{\cdot}7 \times 10^{-56}$ Pa$^{-13/2}$ m$^{-5/2}$ s^{-1}
β_R	$2{\cdot}5 \times 10^{-41}$ Pa$^{-9/2}$ m$^{-5/2}$
γ_C	3×10^{21} Pa$^{5/2}$ m$^{5/2}$
β_C	5×10^{25} Pa^3 m s
k	10^{-9} m^2 s^{-1} Pa^{-1}

DOI: 10.1002/hyp

may be more appropriate to consider the resulting non-dimensional parameters α_C, α_R, κ and δ as the adjustable ones since their physical meaning is also clear.

The values in Table I, along with the typical values $l = 10$ km, $M_0 = 10^{-4}$ m^2 s^{-1}, give rise to the following approximate scalings

$$S_{C0} = 500 \text{ m}^2 \quad S_{R0} = 1{\cdot}3 \text{ m}^2 \quad N_0 = 1 \text{ MPa} \qquad (26)$$

and the values of the non-dimensional parameters are

$$\alpha_C = 0{\cdot}2 \quad \alpha_R = 5 \times 10^{-4} \quad \delta = 0{\cdot}6 \quad \kappa = 10 \qquad (27)$$

A comment on the relevant timescales is in order. α_R gives the timescale for transport in R-channels in years and is, as expected, small. However, when considering transient water flux in a channel the limiting timescale is likely to be the time for the channel area to adjust, which is somewhat longer than the advective timescale. Transient response of a channel is therefore very different to the steady-state behaviour (Clarke, 2003). We will ignore the diurnal changes in melt input and consider only the longer term average which, we assume, varies sufficiently slowly that the channel can be considered to be in steady state. The extra hidden timescale for adjustment of the channel means we should be wary of the importance attached to the value of α_R.

Boundary conditions

We would like to solve (21) and (22) on the region $0 < x < 1$, $x = 0$ being the head of the glacier and $x = 1$ being the terminus. Boundary conditions for this hyperbolic problem are prescribed at the top $x = 0$, and the natural boundary conditions to choose are $Q_C = Q_R = 0$ there. However, the corresponding pressures according to (23) and (24) are unrealistic. In fact, these relationships are incorrect as Q goes to zero, since as this happens the pressure gradients become large and the singular approximation we make in ignoring them breaks down. In order to avoid solving the fuller elliptic problem, which includes these terms, we make the assumption that the region we are interested in starts a little way down from the head of the glacier and the water flux at $x = 0$ is therefore small but finite. In doing so, we ignore a boundary region in which the effective pressure gradient is important; a fuller treatment of this region shows that the pressure tends to a finite value as the flux goes to 0, but the details of this region will depend upon the precise geometry of bed and glacier and we do not go into them here.

For the same reason concerning the neglected effective pressure gradient, we do not attempt to satisfy a condition at the terminus, whereas in the fuller problem we would expect to prescribe that the water pressure be atmospheric and therefore $N = p_i - p_a$. Again, there will be a boundary region in which the pressure adjusts to satisfy this condition.

Relationships between effective pressure and water flux are shown in Figure 2. Under relatively smooth ice, water will locally flow towards regions of high effective pressure where the water pressure is lower. This fact means that water will tend to migrate into the drainage system with the higher effective pressure. For sufficiently large water flux this is the channel system, which therefore captures water from the surrounding cavities, but for very small flux the required water pressure to keep the channels open is large, and the water would flow out into the cavities. Thus, there is a critical water discharge needed in order to keep the channel system open. The simplest criterion as seen from Figure 2 is that $N_R > N_C$ for the same discharge Q, and from (23) and (24) this gives the critical discharge

$$Q_* = \delta^{4n(n+q)/(5n+q)} \qquad (28)$$

Bearing this discussion in mind, we therefore begin by considering the evolution of the two drainage systems by taking the boundary condition

$$Q_C = Q_R = Q_* \quad \text{at} \quad x = 0 \qquad (29)$$

RESULTS AND DISCUSSION

Coupled drainage

Equations (21), (22), (23) and (29) together with (29) are solved numerically using an upwinding forward difference scheme. Figure 4 shows the water flux through the two drainage systems in the steady state when $M_C = 3$ is constant, and shows the increasing fraction of total discharge carried by the channels. To investigate seasonal changes the melt input is again taken to be sinusoidal. Figure 5 shows a contour plot of the spatial and temporal variations in the sliding velocity resulting from the varying cavity pressure. There is a peak at some distance downglacier from the head where the largest water flux is carried by the slow cavity system, resulting in the smallest values of effective pressure. Further down the glacier, the water is carried more and more by the channel system that acts to increase the effective pressure and therefore reduce the sliding velocity.

Seasonal waves

We now attempt to reproduce some of the qualitative features of Figure 1; in particular, we look to explain

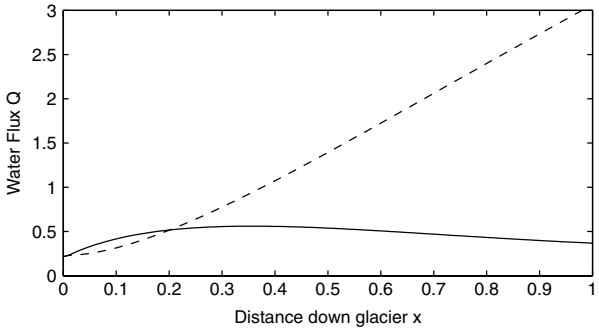

Figure 4. Water flux carried by cavities and channels as a function of distance downglacier. This is the steady-state solution of (21), (22), (23), (24) and (29), with melt input $M_C = 3$. The solid line is the cavity flux, the dashed line is the channel flux

DOI: 10.1002/hyp

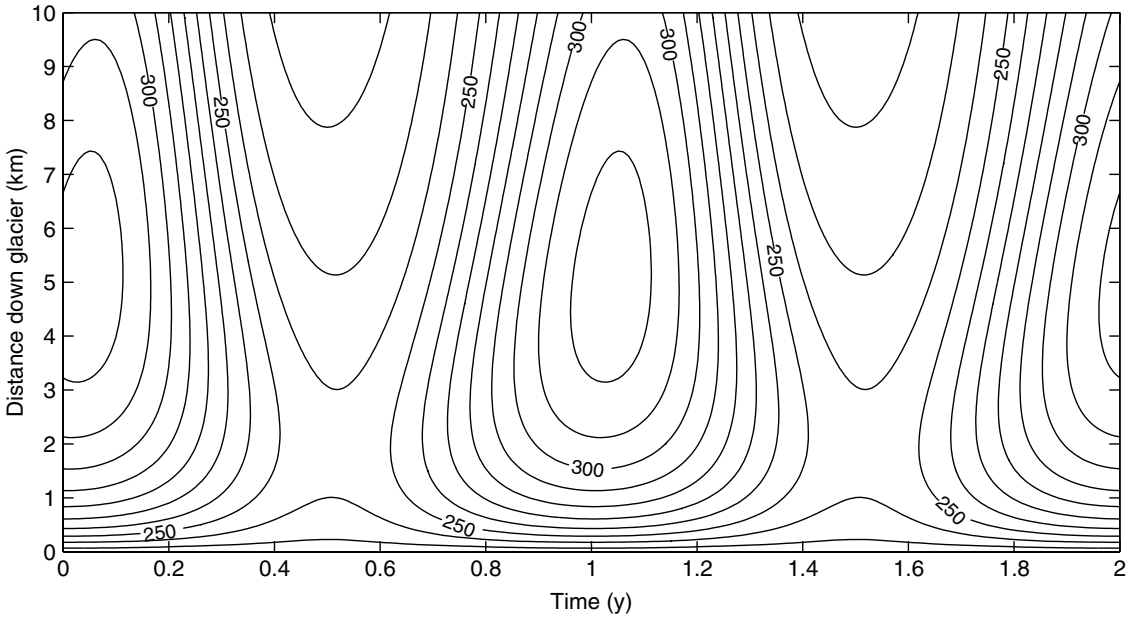

Figure 5. Contour plot of sliding velocity variations due to changing meltwater conditions at the bed, taken from the solution of (21), (22), (23), (24) and (29), using the sliding law (4). Melt input is $M_C = 1 + 2(1 + \cos 2\pi t)$. Contour interval is 10 mm d^{-1}

the seasonal wave (that is, the downstream shift in the timing of velocity minima and maxima), and the general decrease in sliding velocity with distance down the ablation area. The internal deformation velocity of the ice was calculated by Hodge, based on measurements of depth and surface slope. As discussed previously, this changes little throughout the year and it can generally account for only a small component of the surface velocity. The one feature of Figure 1, which may be caused by internal deformation, is the peak in velocities at around 2000 m, which can be attributed to slightly deeper ice and a steeper slope in this region.

We have already seen the possibility for the propagating velocity peaks in Figure 3, but it is seen there that modelled sliding velocities increase all the way to the terminus as the water pressure increases. The observed velocity decrease, which must result through (4) from an *increasing* effective pressure, is exactly what occurs in the lower half of the glacier in Figure 5, which we therefore suggest corresponds to the ablation area in Figure 1.

Equations (21), (22), (23) and (24) are solved again, but we now treat $x = 0$ as the position of the equilibrium line and $x = 1$ as the terminus. The boundary condition (29) at $x = 0$ is therefore replaced with a prescription of the flux of meltwater arriving there from upglacier. This is likely to be non-zero and seasonally varying, so we take a sinusoidal variation, in phase with the varying meltwater input. To aid comparison with Figure 1, the resulting sliding velocity according to (4) is added to the constant deformation velocity, which is calculated using (1) and Hodge's measured depth and surface slope. A contour plot of the surface velocity is shown in Figure 6; the knobbly look is due to slight non-uniformities in the deformation velocity, which, in particular, explains the peak two-thirds of the way down the region.

Several comments can be made on Figure 6 and how it compares with Figure 1. The first is that it demonstrates seasonal velocity changes, with a speed up at all points during the summer when there is maximum melt entering the cavities. The second is that the timing of the peak velocity does move progressively later in the year with distance downglacier. This is the result of the slow passage of water through the cavity system meaning that buildup of cavity pressure occurs later further downglacier. Thirdly, the velocity is generally decreasing towards the terminus, the reason for this being that less meltwater drains through cavities lower down and the cavity pressure is consequently lower there.

Seasonal drainage transition

One feature, in particular, does not agree so well with Figure 1 and that is the apparent 'backward' propagation of the velocity minimum during the winter, of which there is no evidence in Figure 1. This is a result of the capture properties of the R-channels which means that if there is insufficient replenishment of the cavities, the channels suck the water out from them. This points towards a possible fault in the model, which is the presumption that both types of drainage occur throughout the year, whereas most field studies of drainage system evolution suggest that shut down of the channels occurs during the winter when discharge is low (Hooke, 1989; Hubbard and Nienow, 1997; Nienow *et al*., 1998). Drainage is forced to occur through an inefficient distributed system during the winter, before spring melting causes a transition to the efficient channel system.

Our model captures some aspects of this transition in the sense that channels become larger and carry a larger fraction of the meltwater during the summer, but actual shut down of the channels during the winter does not occur. As commented earlier, there is a critical discharge

DOI: 10.1002/hyp

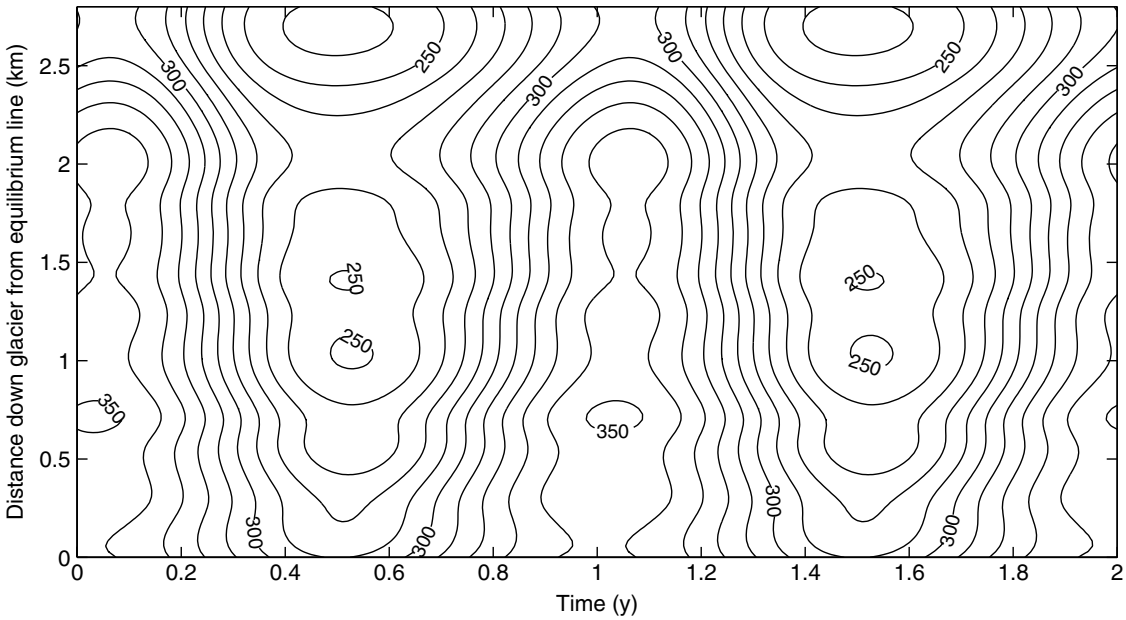

Figure 6. Contour plot of surface velocity variations in the ablation area; the sum of internal motion (1) calculated using measured shear stress, and sliding motion (4) based on modelled subglacial water pressures from (21), (22), (23) and (24), with $M_C = 1 + 1{\cdot}5 \cos 2\pi t$, and $Q_C = Q_R = 0{\cdot}5 + 0{\cdot}25 \cos 2\pi t$ at $x = 0$. Contour interval is 10 mm d^{-1}

required to enable channel drainage to occur and we have assumed that this is exceeded throughout the year, at least in the region we are looking at. The critical value given in (28), based on the condition that water pressure in the channels must be lower than cavities, is indeed small, but this value may be misleading. The suggestion that drainage occurs through a channel if the water pressure is lower than the cavities seems reasonable (e.g. Clarke, 1996), but in order for the channel to exist with that pressure the necessary water flux must be localized in one place, whereas the water in the cavities is widely distributed. Thus, one should expect that the cavity water flux must be significantly larger than (28) in order for a channel to start. A more appropriate criterion for channel initiation is therefore

$$Q_C = Q_{C*} \tag{30}$$

where the value of Q_{C*} will be glacier specific. Microscopic analysis of the unstable transition of cavities into channels (Walder, 1986; Kamb, 1987) suggests transition should occur if cavity pressure is high enough or equivalently, given (9), the cavity discharge is high enough. Field evidence that the transition in drainage occurs with the retreating snowline (Nienow *et al*., 1998) or during periods of warm weather (Anderson *et al*., 2004) when there is a substantial increase in meltwater production agree with this assertion.

To include the transition in our model is relatively straightforward. The glacier is divided into two parts, the upper part in which drainage occurs by cavities only, and the lower part in which both types of drainage occur as above. Thus we have

$$\alpha_C \frac{\partial S_C}{\partial t} + \frac{\partial Q_C}{\partial x} = M_C \quad \text{for} \quad 0 < x < x_T(t) \tag{31}$$

where x_T is the position of the transition where $Q_C = Q_{C*}$, and (21) and (22) still hold for $x_T < x < 1$. The boundary condition at $x = 0$ is $Q_C = 0$, and again in order to ensure that $N_R > N_C$ when the channel system starts, we avoid the details of this initial region by supposing that there is always a small 'fictional' flux Q_{R*} in the channels before they begin;

$$Q_{R*} = \delta^{4n} Q_{C*}^{-4n/(n+q)} \tag{32}$$

Model calculations are made with the melt variation in M_C again taken to be sinusoidal. Somewhat arbitrarily we take $Q_{C*} = 1{\cdot}5$, to ensure that channels close down everywhere during the winter minimum. The resulting pattern of sliding velocity changes is calculated and shown in Figure 7. Also shown in Figure 8(a) are the velocities at four different positions on the glacier, showing that the seasonal variations are very different depending on the position. Figure 7 now looks rather different to Hodge's observations. The top part of the glacier $x < x_T$, in which drainage occurs by linked cavities, suggests that the velocity should increase with distance from the head as the greater water flux requires a higher water pressure. Since this region encompasses the whole length of the glacier during the winter the velocity increases all the way to the terminus. Just as in Figure 3, the slow passage of water during this time produces a seasonal wave in the minimum velocity. In the lower part of the glacier, the transition to channel drainage during the summer has the initial effect of reducing the water pressure so that the sliding velocity reduces, before the large meltwater influx to the cavities in the middle of the melting season has the effect of again overpressurizing the cavities so that there is another peak in the sliding velocity in mid-summer that again propagates downglacier as a seasonal wave.

DOI: 10.1002/hyp

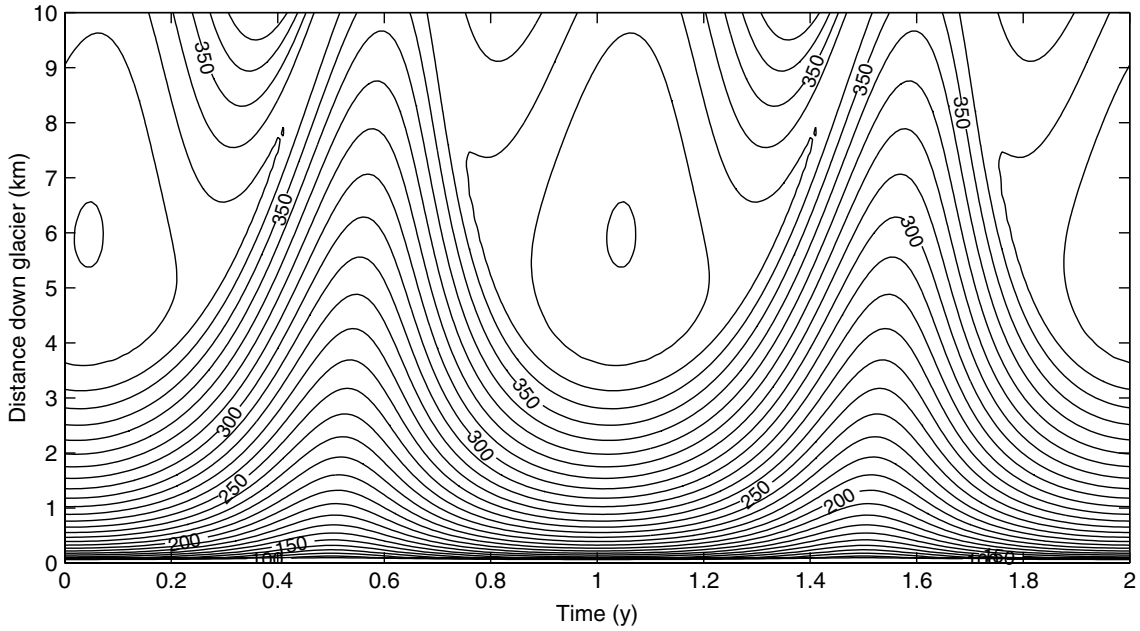

Figure 7. Contour plot of sliding velocity variations with a transition in drainage from linked cavities to a combined system occurring when the cavity discharge reaches $Q_{C*} = 1{\cdot}5$. The position of the transition is roughly equivalent to the 350 mm d^{-1} contour. Velocities are given by the solutions of (31), (21), (22), (23), (24) and (4), with meltwater input $M_C = 1 + 2(1 + \cos 2\pi t)$

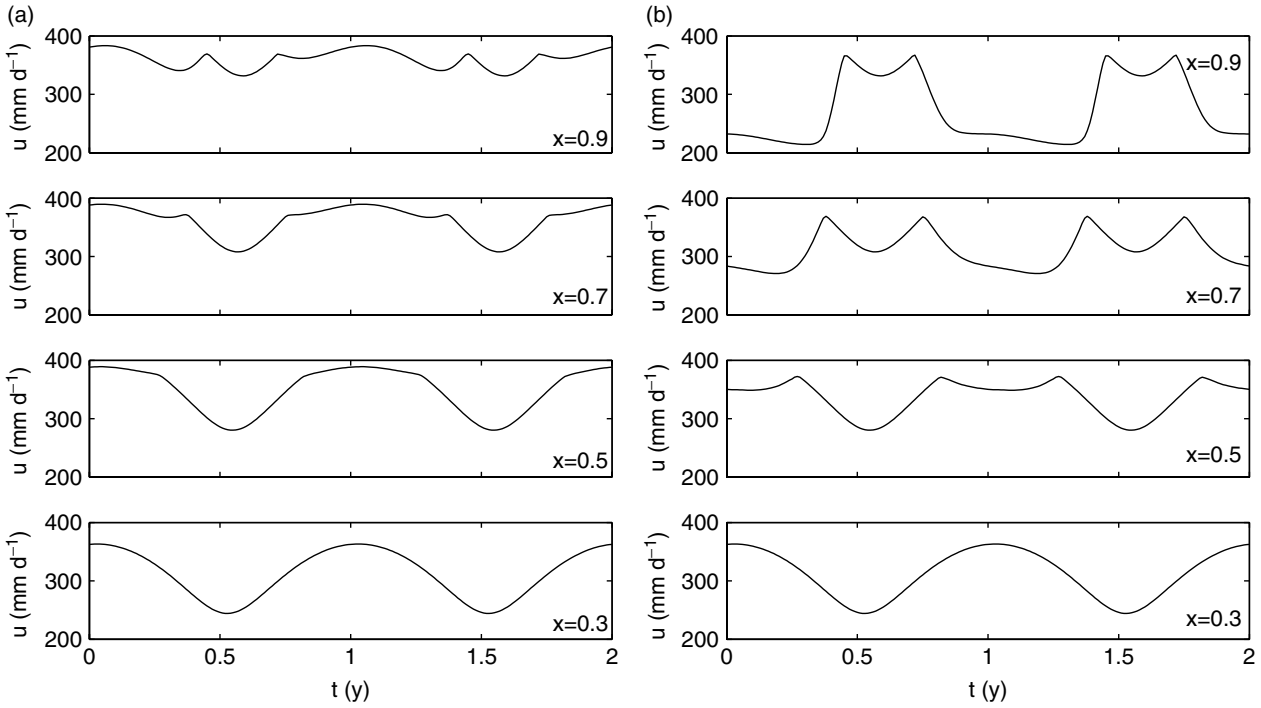

Figure 8. (a) Sliding velocity profiles over 2 years at four points along the glacier, with velocities calculated as in Figure 7. x labels are a fraction of the total length from the glacier head, $t = 0$ corresponds to the time of maximum meltwater input. (b) The same as in (a), but with $\kappa = 20$ rather than 10

This mid-season peak turns out to be heavily dependent on the connectivity parameter κ. If κ is increased, even by a factor of 2, so that water drains more quickly into the channels once they are developed, the situation is very different and is shown in Figure 8(b). At the top of the glacier the picture is broadly similar to Figure 8(a), but lower down in the ablation region the channel drainage in the summer has the effect of reducing water pressures so much that the summer sliding velocity is lower than in winter. There are sharp velocity peaks during the transition periods in spring and autumn that are quite clearly seen to propagate up and downglacier, respectively. The spring speed-up is very similar to that which has been reproduced by Kessler

DOI: 10.1002/hyp

and Anderson (2004) using a similar conceptual drainage model.

It would appear that the same mechanism of meltwater conservation in a coupled drainage system can, depending upon the glacier specific parameter values, produce a peak sliding velocity in mid-summer that propagates slowly as a seasonal wave, or more sharp velocity peaks in the spring and autumn associated with the transition in drainage structure.

Model sensitivity

There is a certain degree of uncertainty in the values of the parameters in this model, and indeed the applicability of the sliding and drainage theories. We have made similar calculations to those above with a range of values for the four non-dimensional parameters, and a range of alternative power laws in the drainage relations (23) and (24). These have reasonably predictable effects on the results. Changing the timescale parameters α_C and α_R alters the delay in water travelling downglacier and therefore alters the 'tilt' seen in the contour plots, changing the speed of the seasonal wave. Increasing δ has a similar effect to decreasing κ since both reduce the tendency for water to move from the cavity system to the channel system. Changing κ has the greatest effect on the results; as discussed above, even a small increase causes water to move quickly so as to equalize the pressures, and the effect, seen in Figure 8, is a rapid decrease in the velocity during the summer as most of the water finds its way into the channels. In this case, there is no seasonal wave in the maximum velocity because the water moves too quickly through the channels.

Altering the power-law relationships between pressure and discharge has little qualitative effect on the results, provided of course the effective pressure still increases with flux in the channels and decreases in the distributed system.

The inclusion of meltwater directly into the channels was also investigated. Since the channels very effectively route out all the water that enters them, this does not make a great difference to the results. What effect it does have is to increase the effective pressure in the channels and therefore make them even more efficient at capturing the water from the cavities.

The coupling L between channelized and distributed drainage systems used in these results has been the straightforward linear dependence on the pressure difference (17). There is evidence to suggest that low pressure channels act to spread the load of the overlying ice to the surrounding regions so that high-pressure 'stress-bridges' form along the edges of the channel, effectively sealing it off from the distributed system (Weertman, 1972; Lappegard *et al*., 2006). In this case, hydraulic communication between the systems is restricted to periods of high pressure when the stress bridge can be overcome, and these will usually be associated with periods of enhanced melting and runoff (Lappegard *et al*., 2006).

This non-linear coupling of the drainage system inherently involves short timescale (diurnal) adjustments of the drainage structures that are not resolved in our model. In our context of smooth seasonally varying melting, we are interested in the longer term average connection between the drainage systems and must therefore choose an appropriate form for L to represent the actual physical processes. One alternative is to include the cavity cross-sectional area in the transmissivity k so that

$$L \propto \frac{1}{N_C^{n+q}}(N_R - N_C) \tag{33}$$

thereby expressing the idea that connection is more efficient when the pressure is high (N_C small) and the cavities open up.

The same model scenarios have been considered with alternative couplings such as (33). These yield results with some differences but without altering the general properties of the seasonal wave and seasonal transitions. Use of (33) causes the two drainage systems to be poorly connected in the winter and can produce a downglacier propagating seasonal wave then as well as in the summer, although the exact pattern of sliding velocities does not well reflect Figure (1).

We refrain from further experimenting with alternative forms for L, since the conclusions are essentially the same and without a more detailed description of the short-term behaviour during transient high-pressure periods, it would detract from the simplicity of the ideas presented here to hypothesize the 'correct' form for L.

Outlook

Figure 6 represents our closest attempt at reproducing the seasonal variations observed by Hodge on Nisqually glacier. The fact that the velocity always decreases significantly from the top to the bottom of the ablation region suggests that effective pressures should be increasing with distance down the glacier and this leads us to the conclusion that some degree of channelized drainage must occur throughout the year. While the passage of a portion of meltwater through the cavity system during summer can produce a seasonal wave then, the channel drainage seems to be incompatible with a seasonal wave in the winter. It might be noted that the waves on the Hintereisferner were observed only during the summer.

The model presented here is straightforward; it is essentially an extension of simple linear reservoir models to include a spatial dependence and some consideration of the physical process by which the water moves through the reservoir, coupled with a power-law sliding law. It is possible that some of the neglected aspects of the model may be important in producing seasonal waves, and further work should look at two principal factors; the neglected pressure gradients in the water potentials $\mathcal{G}$, and the effect of longitudinal stress gradients in the ice. On Nisqually glacier, the region above the equilibrium line is considerably steeper and longitudinal coupling may be a cause of the much higher velocities seen near the top of the ablation region in Figure 1.

DOI: 10.1002/hyp

A more detailed understanding of the seasonal drainage transition, and particularly of the differences between the opening up and closing down of the channelized system, must involve consideration of the channel dynamics (Flowers *et al*., 2004; Kessler and Anderson, 2004). The short-term dynamics may also help to understand to what extent the coupling L really depends on the average properties of the drainage system used here, as well as the magnitude and frequency of large runoff events.

CONCLUSION

Seasonal waves manifest themselves in the progressive shift of a maximum or minimum down the glacier. Kinematic waves in a slow distributed subglacial water system and the accompanying pressure waves are a possible cause of this type of wave, as shown in Figure 6. Working with this hypothesis, one finds that a very slow drainage system, which is poorly connected to any faster channelized system, is necessary to produce the waves; otherwise the presence of the channelized system effectively damps the seasonal peaks in effective pressure, and can lead to an apparent backward wave in which the pressure peak is earlier further downstream.

The speed of the seasonal wave is on the order of the average water speed through the cavity drainage system. To produce the estimated speed on Nisqually glacier requires a drainage timescale of around 1 month. The large decrease in sliding velocity from the equilibrium line to the terminus observed by Hodge is hard to capture with the current model and may point towards some important omissions.

If a seasonal transition in drainage is accounted for, the peak sliding velocity may occur during mid-summer or it may occur during the spring transition in the drainage system, in which case it leads to an upglacier propagation of the velocity peak, as in Figure 8. The same model qualitatively explains both the seasonal wave and the high velocity spring events.

ACKNOWLEDGEMENTS

IJH acknowledges the award of an EPSRC studentship. ACF acknowledges the support of the Mathematics Applications Consortium for Science and Industry (www.macsi.ul.ie) funded by the Science Foundation Ireland mathematics initiative grant 06/MI/005.

REFERENCES

Anderson RS, Anderson SP, MacGregor KR, Waddington ED, O'Neel S, Riihimaki CA, Loso MG. 2004. Strong feedbacks between hydrology and sliding of a small alpine glacier. *Journal of Geophysical Research* **109**: F03005, DOI: 10·1029/2004JF000120.

Blümcke A, Finsterwalder S. 1905. Zeitliche Änderungen in der Geschwindigkeit der Gletscherbewegung. *Sitzungsberichte der Mathematisch physikalischen Klasse der Königlich Bayerischen Akademie der Wissenschaften* **35**: 109–131.

Brzozowski J, Hooke RLeB. 1981. Seasonal variations in surface velocity of the lower part of Storglaciären, Kebnekaise, Sweden. *Geografiska Annaler* **63**: 233–240.

Budd WF, Keage PL, Blundy NA. 1979. Empirical studies of ice sliding. *Journal of Glaciology* **23**: 157–170.

Clarke GKC. 1996. Lumped-element analysis of subglacial hydraulic circuits. *Journal of Geophysical Research* **101**: 17547–17559.

Clarke GKC. 2003. Hydraulics of subglacial outburst floods: new insights from the Spring-Huter formulation. *Journal of Glaciology* **49**: 299–313.

Copland L, Sharp MJ, Nienow PW. 2003. Links between short-term velocity variations and the subglacial hydrology of a predominantly cold polythermal glacier. *Journal of Glaciology* **49**: 337–348.

Deeley RM, Parr PH. 1914. On the hintereis glacier. *Philosophical Magazine* **27**: 153–176.

Finsterwalder R. 1961. Der Haushalt des Hintereisferners (Ötztal). *Journal of Glaciology* **3**: 1159–1160.

Flowers G, Clarke GKC, Björnsson H, Pálsson F. 2004. A coupled sheet-conduit mechanism for jökulhlaup propagation. *Geophysical Research Letters* **31**: L05401, DOI: 10·1029/2003GL019088.

Fowler AC. 1986. A sliding law for glaciers of constant viscosity in the presence of subglacial cavitation. *Proceedings of the Royal Society of London Series A-Mathematical and Physical Sciences* **407**: 147–170.

Fowler AC. 1987. Sliding with cavity formation. *Journal of Glaciology* **33**: 255–267.

Hock R, Hooke RLeB. 1993. Evolution of the internal drainage system in the lower part of the ablation area of Storglaciären, Sweden. *Geological Society of America Bulletin* **105**: 537–546.

Hodge SM. 1974. Variations in the sliding of a temperate glacier. *Journal of Glaciology* **13**: 349–369.

Hooke RLeB. 1989. Englacial and subglacial hydrology: a qualitative review. *Arctic and Alpine Research* **21**: 221–233.

Hubbard B, Nienow P. 1997. Alpine subglacial hydrology. *Quaternary Science Reviews* **16**: 939–955.

Iken A, Bindschadler RA. 1986. Combined measurements of subglacial water pressure and surface velocity of Findelengletscher, Switzerland: conclusions about drainage system and sliding mechanism. *Journal of Glaciology* **32**: 101–119.

Jansson P. 1996. Dynamics and hydrology of a small polythermal valley glacier. *Geografiska Annaler* **78**: 171–180.

Kamb B. 1987. Glacier surge mechanism based on linked cavity configuration of the basal water system. *Journal of Geophysical Research* **92**: 9083–9100.

Kamb B, Engelhardt H. 1987. Waves of accelerated motion in a glacier approaching surge: The mini-surges of Variegated Glacier, Alaska, U. S. A. *Journal of Glaciology* **33**: 27–46.

Kessler MA, Anderson RS. 2004. Testing a numerical glacial hydrological model using spring speed-up events and outburst floods. *Geophysical Research Letters* **31**: L18503, DOI: 10·1029/2004GL020622.

Lappegard G, Kohler J, Jackson M, Hagen JO. 2006. Characteristics of subglacial drainage systems deduced from load-cell measurements. *Journal of Glaciology* **52**: 137–148.

Lliboutry L. 1968. General theory of subglacial cavitation and sliding of temperate glaciers. *Journal of Glaciology* **7**: 21–58.

Lliboutry L. 1969. Contribution à la théorie des ondes glaciaires. *Canadian Journal of Earth Sciences* **6**: 943–953.

Meier MF. 1968. Calculations of slip of Nisqually Glacier on its bed: no simple relation of sliding velocity to shear stress. Union de Géodésie et Géophysique Internationale. Association Internationale d'Hydrologie Scientific. Assemblée générale de Berne, 25 Sept.–7 Oct. 1967. Rapports et discussions, 49–57.

Nienow P, Sharp M, Willis I. 1998. Seasonal changes in the morphology of the subglacial drainage system, Haut Glacier d'Arolla, Switzerland. *Earth Surface Processes and Landforms* **23**: 825–843.

Nye JF. 1960. The response of glaciers and ice-sheets to seasonal and climatic changes. *Proceedings of the RoyalSociety of London A* **256**: 559–584.

Nye JF. 1969. A calculation on the sliding of ice over a wavy surface using a Newtonian viscous approximation. *Proceedings of the RoyalSociety of London A* **311**: 445–467.

Nye JF. 1976. Water flow in glaciers: jökulhlaups, tunnels and veins. *Journal of Glaciology* **17**: 181–207.

Paterson WSB. 1994. *The Physics of Glaciers*. Butterworth-Heinemann: Oxford, UK.

Raymond CF, Benedict RJ, Harrison WD, Echelmeyer KA, Sturm M. 1995. Hydrological discharges and motion of Fels and Black Rapids glaciers, Alaska, U. S. A.: Implications for the structure of their drainage systems. *Journal of Glaciology* **41**: 290–304.

Röthlisberger H. 1972. Water pressure in intra- and subglacial channels. *Journal of Glaciology* **11**: 177–203.
Schimpp O. 1958. Der Eishaushalt am Hintereisferner in den Jahren 1952–53 und 1953–54. Union Géodésique et Géophysique Internationale. Association Internationale d'Hydrologie Scientifique. Assemblée générale de Toronto, 3–14 Sept. 1957. 4, 301–314.
Schoof C. 2005. The effect of cavitation on glacier sliding. *Proceedings of the Royal Society of London Series A-Mathematical Physical and Engineering Sciences* **461**: 609–627.
Shreve RL. 1972. Movement of water in glaciers. *Journal of Glaciology* **11**: 205–214.
Spring U, Hutter K. 1982. Conduit flow of a fluid through its solid phase and its application to intraglacial channel flow. *International Journal of Engineering Science* **20**: 327–363.
Walder JS. 1986. Hydraulics of subglacial cavities. *Journal of Glaciology* **32**: 439–445.
Walder JS, Fowler AC. 1994. Channelized subglacial drainage over a deformable bed. *Journal of Glaciology* **40**: 3–15.
Weertman J. 1957. On the sliding of glaciers. *Journal of Glaciology* **3**: 33–38.
Weertman J. 1958. Travelling waves on glaciers. *IASH* **47**: 162–168.
Weertman J. 1972. General theory of water flow at the base of a glacier or ice sheet. *Reviews of Geophysics and Space Physics* **10**: 287–333.
Weertman J, Birchfield GE. 1983. Basal water film, basal water pressure, and velocity of travelling waves on glaciers. *Journal of Glaciology* **29**: 20–27.
Willis IC. 1995. Interannual variations in glacier motion - a review. *Progress in Physical Geography* **19**: 61–106.
Willis IC, Mair D, Hubbard B, Nienow P, Fischer UH, Hubbard A. 2003. Seasonal variations in ice deformation and basal motion across the tongue of Haut Glacier d'Arolla, Switzerland. *Annals of Glaciology* **36**: 157–167.

DOI: 10.1002/hyp